Project title: Transforming brain surgery by advancing functional-guided neuronavigational imaging

Project acronym: HyperProbe

Grant Agreement: 101071040

Call identifier: HORIZON-EIC-2021-PATHFINDERCHALLENGES-01

D1.1 Lab system development (HyperProbe1)

Leader partner: UNIFI

Author(s): Luca Giannoni, Marta Marradi, Francesco S. Pavone

Work Package: WP1

Due date: Month 12

Actual delivery date: 15/09/2023

Type: DEM

Dissemination level: PU

Tables of contents

Abbreviations

HSI	Hyperspectral Imaging
NIR	Near Infrared
HbO_2	Oxyhaemoglobin
HHb	Deoxyhaemoglobin
CCO	Cytochrome-C-Oxidase
SCL	Supercontinuum Laser
AOTF	Acousto-Optics Tuneable Filter
FWHM	Full-Width Half Maximum
sCMOS	Scientific Complementary Metal-Oxide Semiconductor
QE	Quantum Efficiency
SNR	Signal-to-Noise Ratio
NAD/NADH	Nicotinamide Adenine Dinucleotide
FAD	Flavin Adenine Dinucleotide
5-ALA	5-Aminolevulinic Acid
FOV	Field Of View
GUI	Graphical User Interface
UV	Ultraviolet

LED	Light-Emitting Diode
PLS	Plasma Light Source
FWS	Flexible Wavelength Selector
LGG	Low-Grade Glioma
HGG	High-Grade Glioma
PBS	Phosphate-Buffered Saline
ROI	Region Of Interest

Disclaimer

1. Introduction

The deliverable presents the design, development and assembling of a fully-working setup for the laboratory version of the HyperProbe system, named **HyperProbe1**. The main objective and target of the deliverable was to deliver a laboratory-scale, top-grade hyperspectral imaging (HSI) instrument that enables maximum flexibility in the use of variable numbers and types of wavelengths across the visible and near infrared (NIR) range, as well as employs cutting-edge technology for illumination, spectral separation, detection of light, as well as image collection and reconstruction.

HyperProbe1 is intended to be a key first step for calibrating and optimising the performances of the subsequent clinical prototypes (HyperProbe2 and 2.1), such as number/type of wavelengths to be used or optimal illumination power, and to test the capabilities of the system to target the biomarkers of interest in neuronavigation (e.g., oxy- and deoxyhaemoglobin (HbO_2, HHb), cytochrome-c-oxidase (CCO), among others), as well as its biocompatibility and medical safety. This will be done in the future *in vivo* on animal models (murine) and *ex vivo* on fresh surgical biopsies of both healthy and tumour brain tissue. The HyperProbe1 will also be employed to develop the initial version of the software for the data analysis and image reconstruction. Afterwards, the results obtained with the laboratory instrumentations will be used to identify the essential features that allow the desired, application-tailored imaging performances of the final HyperProbe device, in the light of its down-scaling and translation within the surgical room for neuronavigation during glioma resection, defining in this way the starting point of the following clinical prototypes (HyperProbe2 and 2.1).

2. Design of HyperProbe1 system

2.1 Spectral selection and illumination

The design of HyperProbe1 is based on the use of a **supercontinuum laser (SCL) source** that emits a broadband light at high power density across a large portion of the electromagnetic spectrum. A SCL source was chosen since it is the type of optical technology that currently provides the highest spectral radiance ($W \cdot m^{-2} \cdot sr^{-1} \cdot nm^{-1}$) in commerce and it is also been largely applied in HSI and similar diffuse optics techniques [1–3].

The SCL was then coupled with **acousto-optical tuneable filters (AOTF)**, to modulate the broadband light and separate it in its constituent spectral components. AOTFs allow the user to select any narrow spectral band (with bandwidth down to 1-2 nm, FWHM) from the broad spectrum emitted by the SCL, as well as to freely modulate its intensity. They guarantee high transmittance (more than 85%), and are also capable of fast switching between adjacent spectral bands (with switching speed down to 10-100 µs), so that the target can be illuminated rapidly at different wavelengths sequentially. At the current state, they provide the fastest method for spectral filtering in commerce [1,2].

The combination of rapid tuneable filtering, provided by AOTFs, with high-power, broadband illumination from SCL can effectively allow HSI with small exposure times (in the order of tens of ms), thus achieving hyperspectral rates with large numbers of wavelengths (e.g., 50 to 100) within second, or even sub-second, temporal resolution [2].

2.2 Light detection and image reconstruction

A **scientific complementary metal-oxide semiconductor (sCMOS) camera** was then chosen to acquire images of the target at each illuminating spectral band, in order to reconstruct a 3D spatio-spectral dataset, called ‘hypercube’. The ‘hypercube’ contains the full scale of the optical signature of the target and its analysis can provide full characterisation of the morpho-chemical features of the imaged object [2,4]. sCMOS cameras combine fast frame rates (tens to hundreds of fps) with high dynamic ranges. In particular, for HyperProbe 1, a high-format, high-resolution sCMOS camera with adequate quantum efficiency (QE) also in the NIR range

was targeted, in order to maximize both spatial resolution and signal-to-noise ratio (SNR).

As the fluorescence signature emissions of biomolecule of interests [2], such as autofluorescent nucleotides (e.g., NAD/NADH) and flavoproteins (e.g., FAD), as well as of routinely injected contrast agents and tumour markets in surgical practice (e.g. fluoresceine and 5-ALA [5]), are also one of the investigated targets of the HyperProbe device, we envisioned the integration of the imaging camera with a **motorised filter wheel** equipped with various emission filters. These emission filters are designed to isolate the emission signature of the targeted fluorophores. The control of the motorised filter wheel allows to add additional frames to the spectral scanning that indeed targets fluorescence signals, instead of diffuse reflectance.

2.3 Additional instrumentation

Besides the core components described in the previous sections, additional optical devices were essential to be integrated for the final completion of the HyperProbe1 setup. These supplementary optical accessories were: (1) one or more apochromatic or reflective objectives (and conjugated imaging relay lenses), to couple with the camera for achieving the desired magnifications and minimising chromatic aberrations; (2) a laser speckle reducer, to minimise the occurrence of speckle patterns in the illumination light; (3) a laser amplitude stabiliser, to maintain the laser output adequately constant over time; (4) a polariser lens to eliminate unwanted specular reflection; and (4) optic fibres to deliver the light to the desired target.

A schematic diagram for the final design of HyperProbe1 is reported in Figure 1.

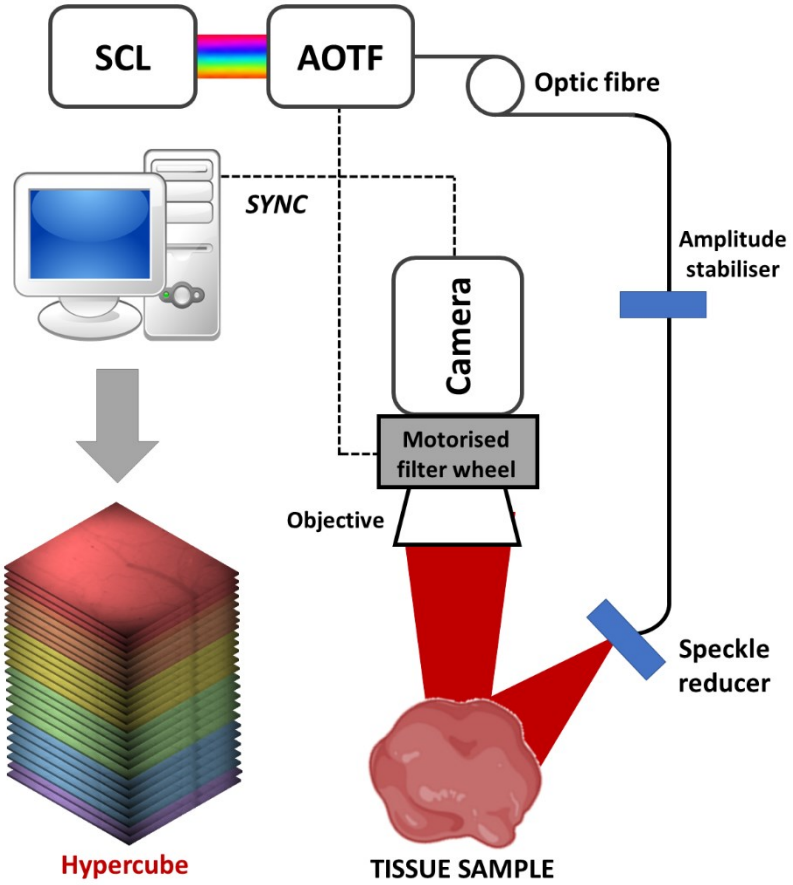

Fig. 1. *Schematics of the design of HyperProbe1 with all its components.*

3. Development of HyperProbe1 system

Based on the design of choice previously described, several items were selected and/or purchased, according to allotted budget and key performances. A review of each of these components is reported in Table 1.

Tab. 1. *List of components of the HyperProbe1 setup with key features.*

Component	Manufacturer & model	Key specifics
SCL	NKT Photonics, SuperK FIANIUM FIR20 [6]	Broadband illumination (400-2400 nm); Maximum total power of 6.5 W;
AOTF	NKT Photonics, SELECT VIS-nIR [7]	Broadband selection (500-900 nm); Spectral resolution of 3.5 nm;
Camera	PCO, pco.panda 4.2 [8]	4.2-MP (2048 x 2048) sensor; 6.5-µm pixel size; QE up to 80% (Visible and NIR); Maximum frame rate of 40 fps;
Filter Wheel	Cairn Research, Dual OptoSpin32 [9]	Up to 10 filter allocations; Stepping time between filters of 40-70 ms;
Amplitude stabiliser	Thorlabs; NEL02A/M + NEL03A/M [10]	Amplitude stabilization within ±0.05%;
Speckle Reducer	Optotune; LSR-3005-6D-NIR [11]	Transmission up to 98%;
Optic fibre	NKT Photonics, SuperK CONNECT [12]	Broadband coverage (400-2000 nm); High power throughput (up to 500 mW); 1-mm core diameter;
Objective 1	Olympus, SDF PLAPO 1X PF [13]	1x apochromatic macro objective; FOV of 1x1 cm^2;
Objective 2	Thorlabs, LMM15X-P01 [14]	15x reflective objective; FOV of 1x1 mm^2;

The HyperProbe1 system is depicted in Figure 2, showing all its main components. The setup is composed of a SCL (NKT Photonics, SuperK FIANIUM FIR20 [6]), generating a coherent, broadband illumination (400-2400 nm) at a maximum total power of 6.5 W, and a set of AOTF (NKT Photonics, SELECT VIS nIR [7]) that selectively filter any desired spectral band between 510 and 900 nm, with a minimum bandwidth of 3.5 nm (FWHM). The filtered light from the AOTF is directed to the sample through an optic fibre delivery system (NKT Photonics, SuperK CONNECT [12]) coupled with: (1) a pair of laser amplitude stabiliser (Thorlabs; NEL02A/M and NEL03A/M [10]), to eliminate intensity noise and maintain illumination stable over time within 0.05% of a selected output power, (2) a laser speckle reducer (Optotune, LSR-3005-6D-NIR [11]), and (3) an achromatic doublet lens, to make the beam divergent in order to obtain an illumination spot of 2-3 cm^2 on the target. Image acquisition at each spectral band is obtained using a high-format (4.2 MP), high-resolution (6.5-µm pixel size) sCMOS camera (PCO, pco.panda 4.2 [8]) capable of acquiring at up to 40 fps of frame rate. The associated optics are composed of two interchangeable objectives (and conjugated tube lens): (1) an apochromatic, 1x macro objective, that generates a field of view (FOV) of about 1x1 cm^2; and (2) a reflective, 15x objective, that produces a FOV of about 1x1 mm^2, according to the specific application involved that may require a larger or smaller magnification, respectively. Finally, a motorised filter wheel is located between the objective and the camera assembly, for automatic selection of up to 10 emission filter slots (25-mm diameter) with switching speed between 40 and 70 ms. The emission filter will be chosen during the preliminary testing of the system, depending on the investigated fluorophores of interest.

3.1 Operational overview of HyperProbe1

The HyperProbe1 can normally scan the entire spectral range of operation (500-900 nm) by sampling sequentially 80 wavelength bands at 5-nm steps. This allows sufficient separation

Funded by the European Union
European Innovation Council

between the bands and avoid major overlapping, based on the spectral resolution of the AOTF (3.5 nm, FWHM). Each spectral band is also modulated in amplitude by the AOTF, in order to provide an approximately constant output power at the illuminated target of about 200-300 µW per band. This is aimed at maintaining a fixed integration time of the camera for each spectral frame (in the order of 5 to 30 ms, depending on the target), as well as an adequate SNR throughout every acquired hypercubes. The typical acquisition time for an entire hypercube (80 bands) ranges between 0.5 to 2 s.

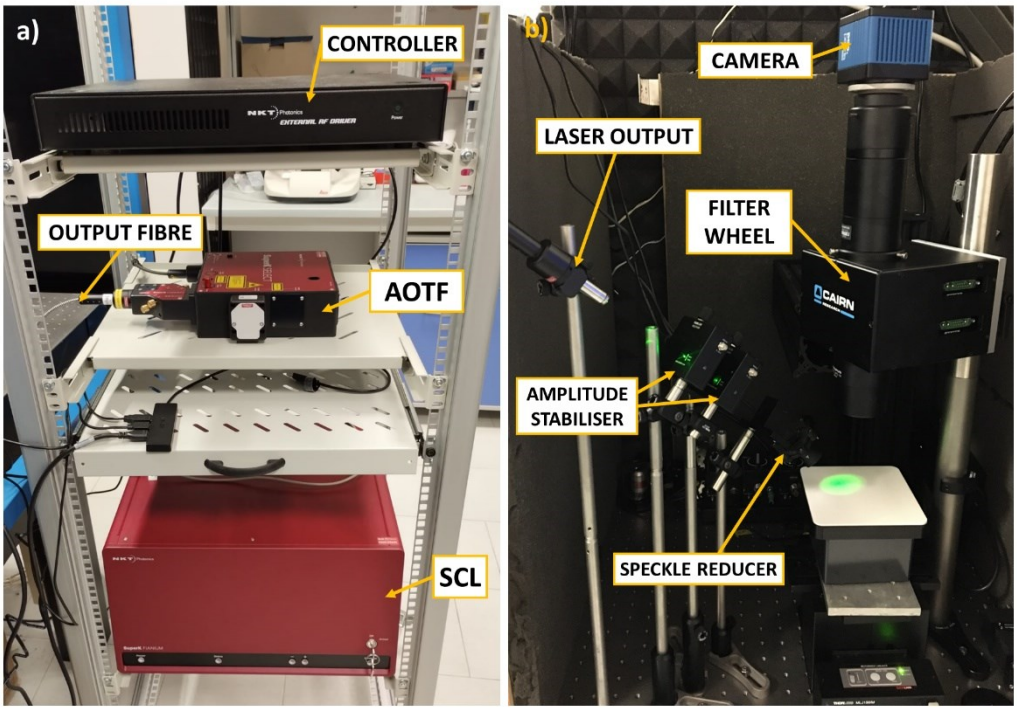

Fig. 2. *a) Picture of the spectral illumination side of the HyperProbe1 setup; b) Picture of the imaging and detection side of the HyperProbe1 setup.*

The entire hyperspectral scanning and image acquisition process, as well as the operational routine of HyperProbe1, are all controlled via a custom-made, graphical user interface (GUI) software, based on LabVIEW [15].

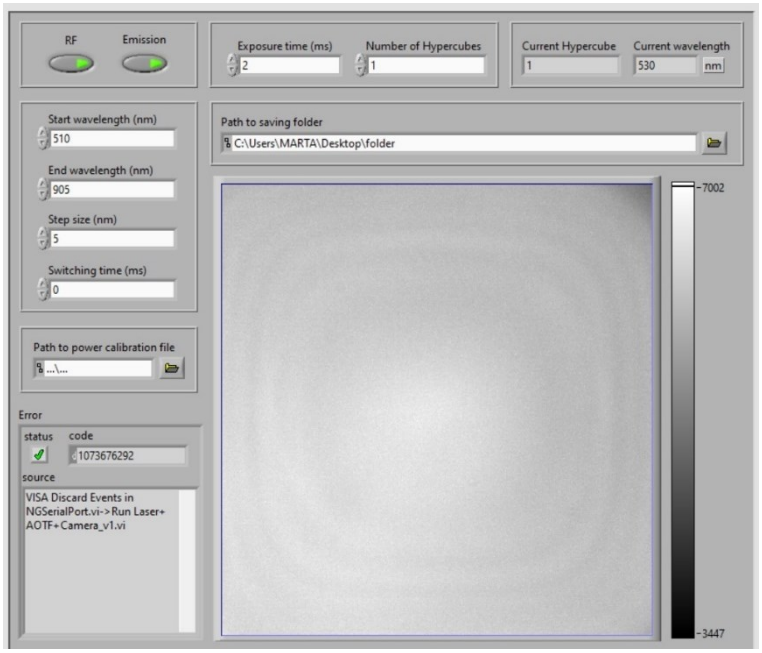

Fig. 3. *Depiction of the custom-made, LabVIEW-based software used to run and control HyperProbe1.*

Funded by the European Union
European Innovation Council

Comprehensive, detailed preliminary testing and technical characterisation of the key performances of the HyperProbe1 system (e.g., quantification of spectral power density, spectral resolution and sampling, imaging spatial resolution and SNR, temporal resolution and imaging acquisition rate) will be conducted in the period M12-M18, as part of Task 1.3 of WP1, and reported in Deliverable D1.2 at the end of M18.

3.2 Laser amplitude stabilisation

Power output stability over time and noise in the spectral illumination were two major issues in the development of HyperProbe1. SCL typically have a power stability of about ±1% (generally worse than both conventional lasers and also non-coherent sources [1]) including the model employed in the HyperProbe1 setup, and over period of times, in the order of tens of minutes to hours, their power output tends to oscillate. Such oscillations in amplitude can be significant, especially within the context of repeated spectral scanning illumination, with the risk of equivalent spectral bands having a non-negligible difference in base intensity over repeated scans. This can lead to discrepancies in the data of the hypercubes over time, that do not depend on actual changes in the optical properties of the target, thus producing errors when retrieving the spectral signatures of the chromophores of interest.

Stabilisation of the SCL power output was therefore a critical step in the development of HyperProbe1, that we aimed at solving by employing laser amplitude stabilisers (also known as “noise eaters”). This type of devices are composed of a feedback loop that feeds a small percentage of the incoming laser light to a photodiode, to constantly monitor its amplitude oscillations. The feedback loop then acts on a modulation module (in the case of the laser amplitude stabilisers used in the HyperProbe1 setup, this is composed of a liquid crystal retarder and a polariser [10]), that adjusts the transmitted laser beam in order to maintain the power output constant (within 0.05%). However, laser amplitude stabilisers in commerce do no cover a broad portion of the electromagnetic spectrum (either the visible or the NIR only). Hence, we decided to first test individually two amplitude stabilisers (Thorlabs; NEL02A/M and NEL03A/M [10]) that operates in the range 425-650nm and 650-1050 nm, respectively, and then tried to combine the two together to optimise their performances.

The first test was performed with the NEL03A/M, renamed “Noise Eater 1”, operating between 650 and 1050 nm. A series of reflectance spectra were acquired with HyperProbe1 equipped only with Noise Eater 1 on a white calibration standard (Labsphere, Spectralon® 5" [16]), after dark count subtraction, at intervals of 10 min between each other for a total 1 hour. The results are shown in Figure 4a.

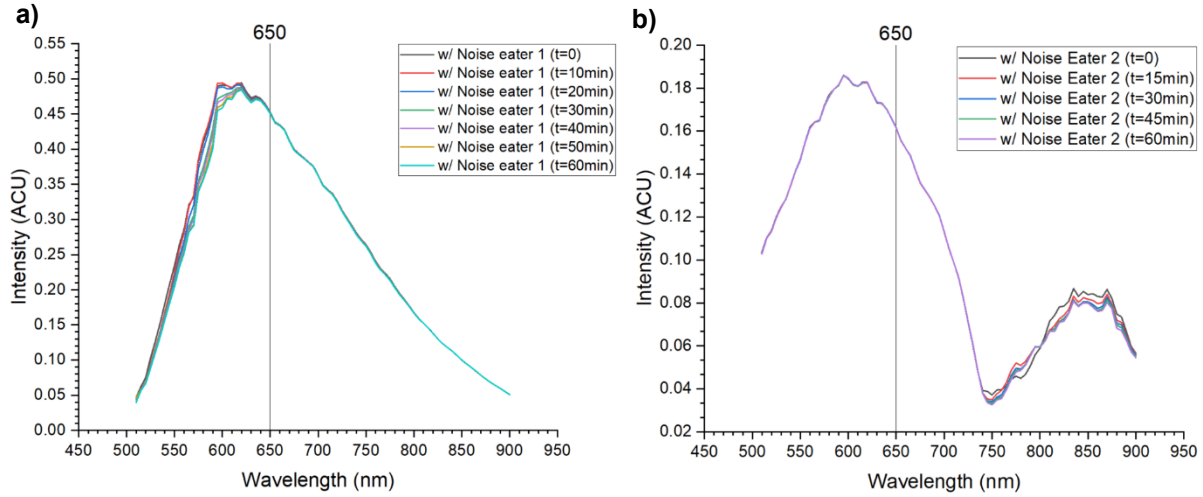

Fig. 4. *Series of reflectance spectra acquisitions with HyperProbe1 equipped with either Noise Eater 1 (NEL03A/M) and b) Noise Eater 2 (NEL02A/M), to test amplitude stabilisation.*

Funded by the European Union
European Innovation Council

The results of the acquisitions shows that the Noise Eater 1 is effective at minimising laser amplitude oscillations above 650 nm over the whole duration of the test, as expected, whereas significant differences (up to 10%) in the spectra are reported below 650 nm, outside of the operating range of the device. Afterwards, a similar test was performed with HyperProbe1 equipped only with the NEL02A/M, renamed “Noise Eater 2” and whose operating range spans between 425 and 650nm. Again, a series of reflectance spectra were acquired on the same white calibration standard after dark count subtraction, at intervals of 15 min between each other for a total 1 hour. The results are shown in Figure 4b. Oppositely to Noise Eater 1, Noise Eater 2 stabiles the output power of the laser over time up to about 750 nm (even a little above its operating range). However, this comes at cost of a drastic reduction in power between 650 and 750 nm. Above 750 nm, significant oscillations (up to 5-7%) in the reflectance spectra are again reported, as well as a slightly higher power transmission.

The final test involved the combination in series of the two devices (i.e., Noise Eater 2 and 1) to cover the entire spectral range of HyperProbe1. Again, a series of reflectance spectra were acquired on the same white calibration standard after dark count subtraction, at intervals of 10 min between each other for a total 1.5 hours. Figure 5 shows the results of this final test.

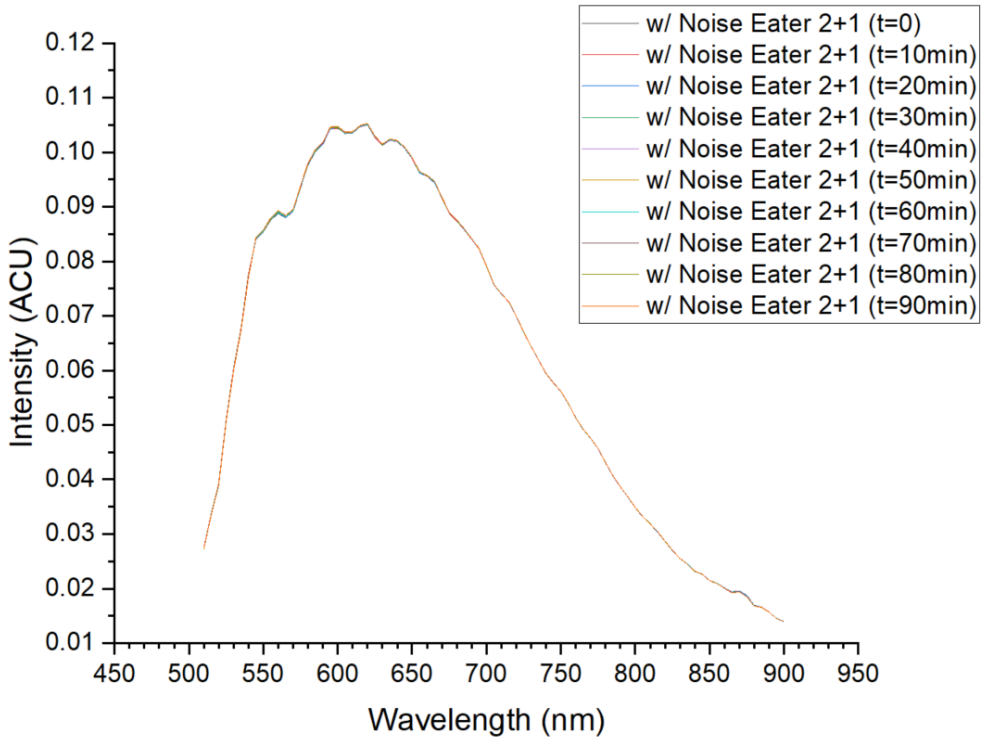

Fig. 5. *Series of reflectance spectra acquisitions with HyperProbe1 equipped With both Noise Eater 2 (NEL02A/M) and Noise Eater 1 (NEL03A/M) in series.*

The combination of the two laser amplitude stabiliser is shown to be effective at reducing below significance any oscillation in the illuminating power of the HyperProbe1 system at the target, for the whole duration of the test (which is order of the maximum duration of any planned experiment with HyperProbe1) and across the entire spectral range of the setup.

3.2 Limitations of the current HyperProbe1 setup

A number of limitations and drawbacks in the current design of HyperProbe1 has been highlighted during the assembly and preliminary testing of the setup. In particular, in the previous chapter we showed the impact of the limited stability over time of the SCL and the mitigation measures we implemented. Despite achieving a stabilisation within 0.05% of the desired output by using two laser amplitude stabilisers in series, the configuration is quite cumbersome and not ideal, due to the lack of full coverage of the spectral range of the system by a single

device. Furthermore, such stabilisation comes at the cost of a reduction in the total output power of the system of about 5 times (as seen in Figure 4 and 5), due to operating both stabiliser outside of their working range with diminished transmission. A possible solution for this would be to adopt a configuration where the two laser amplitude stabilisers operate in parallel, instead of series, by splitting the SCL output with a dichroic mirror in two separate beams (each composed of light only within the operating spectral range of the corresponding noise eater it is directed towards) before entering the devices and then recombining the beams afterwards. However, such configuration is much more complicated than the current one and it is associated with other issues and difficulties, such as the alignment and recombination of the beams, as well as the selection of a dichroic mirror with a cut-off wavelength that satisfies the requirements of both noise eaters.

A second limitation of the current HyperProbe1 system concerns the operating spectral range of the AOTF, which currently only cover between 500 and 900 nm, thus excluding both the shorter section of the visible range (400-500 nm) and also the near ultraviolet (UV), below 400 nm. Both intervals are of substantial importance, since the former involves predominant absorption from both forms of haemoglobin [17], whereas the latter includes fluorescence peaks from potential fluorophores of interest [2]. In addition, the range above 900 nm could also provide valuable information about the absorption properties of water and lipids [17]. Current AOTF technology on the market lacks simultaneous coverage of all the abovementioned ranges of the electromagnetic spectrum.

Finally, spectral selection via AOTF do not allow the user to change the bandwidth of the desired wavelengths. Such aspect can be beneficial for the HyperProbe1 setup, as increasing the bandwidth of the spectral bands beyond the limit of the spectral resolution can be used to simulate other types of light sources, such as filtered light-emitting diodes (LED), that typically have bandwidths of 10 to 20 nm (FWHM). The latter is a type of light technology that could be envisioned for downscaling HyperProbe1 to the future clinical prototypes (HyperProbe2 and 2.1), thus testing LED-like illumination with the laboratory setup can be advantageous for WP2.

3.3 Next steps in the development of HyperProbe1

Taking into account the current technical limitations (as described in the previous section), a number of upgrades has been envisioned for HyperProbe1 to finalise and optimise its development. In particular, alternative instrumentation for the spectral illumination has been purchased to enhance power stability and filtering flexibility of the setup. The complementary illumination design is composed of a broadband **plasma light source (PLS)**, which is a type of coherent light source that is driven by a laser-induced plasma. Such process permits to achieve a much higher spectral radiance for a coherent source over a large portion of the electromagnetic spectrum, that is comparable with that of a SCL, yet without the disadvantage of generating laser speckle and at a greater power stability over time. The PLS is then coupled with a **flexible wavelength selector (FWS)** based on TwinFilm™ technology [18], which combines two rotating broadband bandpass filters for versatile selection of any desired spectral band and adjustment of its bandwidth (compared to AOTF, where the bandwidth is fixed). The FWS also provide a larger spectral operating range, as well as higher efficiency and repeatability than AOTF. The only disadvantages of such new instrumentation, compared to the current one already employed by HyperProbe1, are: (1) the need to optically collimate the output of the PLS source to avoid power losses (whereas a SCL is already a collimated source by its nature); and (2) the lower spectral scanning time of the FWS to switch between wavelength bands (in the order of ms, compared to µs for the AOTF). Even so, the latter does not represent a limitation for the performances of HyperProbe 1, since it can still guarantee a temporal resolution in the acquisition of the hypercubes that stands at a few seconds (thus, very close to real-time imaging for a single hyperspectral, full dataset). The new components selected for the complementary spectral illumination configuration are described in Table 2, highlighting their key characteristics and features.

Tab. 2. *New components for the upgrade of HyperProbe1 with their key features.*

Component	Manufacturer & model	Key specifics
PLS	Isteq, XWS-65 [19]	Broadband illumination (250-2500 nm); Spectral radiance up to 68 $mW \cdot m^{-2} \cdot sr^{-1} \cdot nm^{-1}$; Output power stability less than 0.15%;
FWS	Spectrolight, FWS-Poly-CUS-10 [20]	Broadband selection (385-1015 nm); Variable bandwidth selection (3-15 nm); Band switching time between 10 and 100 ms;

For the source, a PLS model (Isteq, XWS-65 [19]) with broadband coverage between 250 and 2500 nm has been selected, capable of producing a stable output (less than 0.15% variance over time from the expected power) with spectral radiance up to 68 $mW \cdot m^{-2} \cdot sr^{-1} \cdot nm^{-1}$. The tuneable filter is an automatically-adjustable FWS (Spectrolight, FWS-Poly-CUS-10 [20]) that can extend the spectral range of HyperProbe1 to 385-1015 nm, thus including also near UV, all the visible and extending the NIR coverage. It also allow the user to freely vary the bandwidth of the selected wavelengths from 3 to 15 nm (FWHM), thus enabling the simulation of several filtered-LED sources. The FWS can switch between adjacent (5-nm steps) spectral bands in less than 10 ms and takes about 100 ms to span the entire operational range. Finally, another great benefit of these new devices is also that they can act independently and be mixed-and-matched with the current instrumentation, such as combining the SCL with the FWS. This feature can be significantly explored in the future to fully optimise the HyperProbe1 setup in an incredibly versatile way.

The new instrumentation has been currently purchased and it is expected to be delivered by M13-14. Assembly, integration within the current HyperProbe1 setup and testing will then follow accordingly, and be reported in Deliverable D1.2.

4. Preliminary investigations on surgical biopsies

The current setup of the HyperProbe1 (described in Section 3) has been used to start preliminary investigations and testing on fresh *ex vivo* samples of glioma from surgical biopsies, to analyse the initial performances of the system and work towards providing a fully optical, spectral characterisation of cerebral tumoral tissue, as an anticipation to Task 1.4. Such broad-range, optical characterisation of glioma samples is aimed at producing a more objective, comprehensive and quantitative insight in the spectro-chemistry of the tumour itself and help identifying novel biomarkers for cancer imaging via HSI.

The results of these investigations have been presented at the 2023 European Conference of Biomedical Optics in Munich, Germany, on June, 26, 2023, and later published as conference proceedings on August 2023 [21]. Parts and figures of the of the conference proceeding [21] by L. Giannoni *et al* have been modified and adapted to form parts of this section, with reprint permission under CC BY 4.0 License.

4.1 Methods and materials

The current HyperProbe1 system was employed at full capacity (as described in Section 3 and 3.1), acquiring reflectance spectra of the biopsies at sequentially 80 wavelength bands between 500 and 900 nm, at 5-nm steps. The reflective objective was used for this application, given the size of the samples, focusing on a FOV of 1x1 mm^2. However, due to low SNR in the data the two bands at 505 and 510 nm were discarded for this study.

Spectroscopic analysis of the sample was also performed using a laboratory spectrophotometer, to extend the spectral coverage down to 400 nm, as well as to compare and cross-match

part of the results obtained with HyperProbe1. The laboratory, high-resolution, reflectance spectrophotometry setup (Figure 6a), is composed of: (1) a broadband, tungsten-halogen light source (Ocean Insight, HL-2000 [22]) with nominal power up to 20 W, (2) a compact spectrometer (Ocean Insight FLAME [23]) with high signal-to-noise ratio (300:1), (3) a bifurcated, dual fibre that delivers the light to the sample with an annular bundle configuration and collect the reflected light from a central core to the spectrometer, and (4) a sample holder that allows to illuminate the target biopsies from below. The spectrophotometer setup is capable of acquiring full reflectance spectra in a range spanning from 400 to 600 nm, with spectral resolution of approximately 0.2 nm, thus completing the coverage of the visible range below the 510 nm limit of the HyperProbe1 system.

The glioma samples (Figure 6b) were obtained from fresh surgical biopsies of patients taken during routinely performed glioma resection neurosurgery at the partner **Azienda Ospedaliero-Universitaria Careggi**. They were composed of the same glioma tissue removed from the resection that is typically sent to laboratory histopathological analysis. Samples of both low-grade (LGG) and high-grade glioma (HGG) have been analysed. The samples were preemptively washed and stored in phosphate-buffered saline (PBS) solution for transportation, to prevent deterioration and oxidation of the tissue.

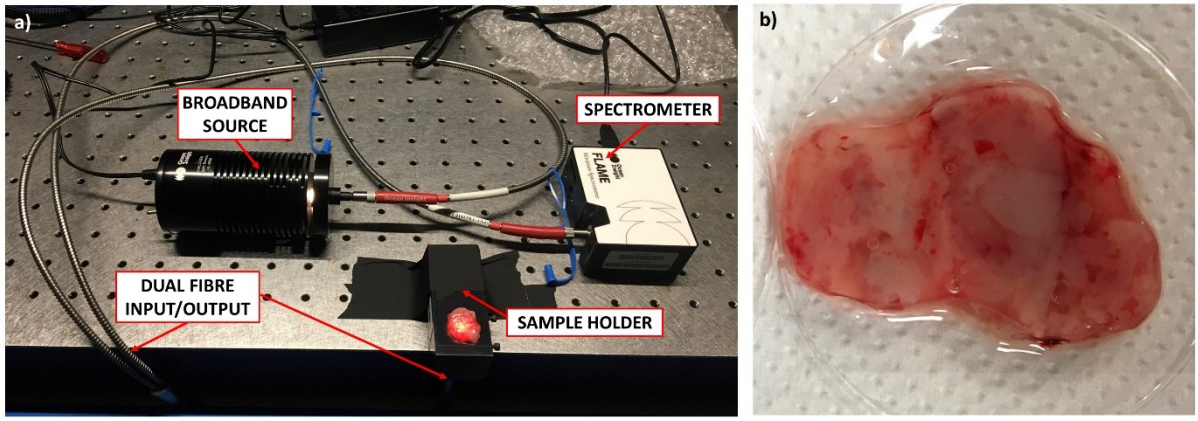

Fig. 6. *a) Picture of the laboratory spectrophotometer; b) Example of ex vivo glioma biopsy.*

For the HSI data acquisition, a portion of the glioma samples was removed from the PBS solution and imaged on its surface using the HyperProbe1. A thin glass coverslip was placed over the sample to flatten its top surface, in order to better maintain the whole FOV in focus. The acquisition of a single hypercube took less than 2 seconds, which was a duration short enough to ensure that the samples had not deteriorated or oxidised during the imaging. Full reflectance spectra were then reconstructed for each pixel of the FOV on the samples by normalising the hyperspectral data with a reference spectrum obtained using the white calibration standard, after dark counts subtraction.

For the spectroscopic analysis, the same portion of the glioma is turned over the coverslip and placed on the sample holder of the spectrophotometer setup. This way, the same region of the surface of the sample imaged with HyperProbe1 is also sampled with the spectrophotometer. For each sample, 10 spectra acquired for 25 ms each were averaged using a boxcar filter of unitary width. Full reflectance spectra were then reconstructed by normalising the averaged data with a reference spectrum obtained using the same white calibration standard as for the HSI data, after dark counts subtraction.

A total number of 5 samples (n = 5) were analysed with both the HyperProbe 1 system and the spectrophotometer, of which 2 were LGG and 3 were HGG, to guarantee a degree of statistical robustness in the reconstructed spectra and to investigate specimen and spatial variability across the samples.

4.2 Results

We expect the datasets of spectra from the combination of the HSI acquisition and the spectrophotometer to be primarily influenced by the scattering properties of the diffusive brain tissue in the visible and NIR, as well as by the absorption features of both HbO_2 and HHb, as the two major chromophores [2]. In particular, the absorption from haemoglobin is predominant and mainly shape the spectra in the visible range, with features connected to biomarkers of blood oxygenation and perfusion within the tissue, identifiable at the peaks corresponding to haemoglobin at about 540 and 575 nm for HbO_2, and 555 nm and 755 nm for HHb. Also, the contribution from water and lipids may also have an influence to the spectral signatures for the longer wavelengths, above 850 nm. Absorption spectra for HbO_2 and HHb (assuming 150 g/L concentration of haemoglobin in blood and blood volume content in generic brain tissue equal to 5%) are reported in Figure 7a, together with the absorption spectra of pure water and lipid, as well as the scattering properties of generic brain tissue [17]. Furthermore, the presence of CCO, an enzyme directly involved in aerobic respiration and cellular metabolism [24], could be a potential novel biomarker for differentiating glioma samples that have never been targeted and investigated before. The redox states of CCO have specific optical signatures, which become predominant absorbers in the NIR portion of the electromagnetic spectrum, between 780 and 900 nm (Figure 7b), and thus also have an influence on the shape of the spectra in such range. We decided therefore to focus our analysis particularly on such chromophore.

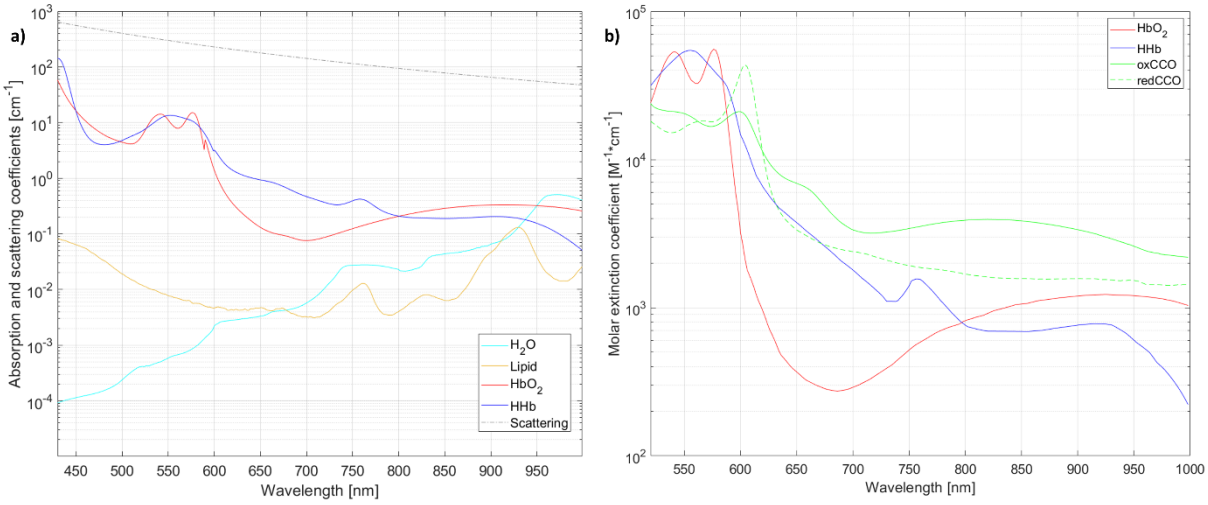

Fig. 7. *a) Absorption coefficients for HbO_2, HHb, lipid and water, and scattering coefficient of generic brain tissue in the visible and NIR range (150 g/L concentration of haemoglobin in blood and blood volume content in Generic brain tissue equal to 5% are assumed); b) Molar extinction coefficients Of HbO_2, HHb, oxCCO and redCCO in the visible and NIR range.*

An example of processed hyperspectral image collected with HyperProbe1 on a HGG sample is depicted in Figure 8a, for a bandwidth centred at 560 nm. Different regions of interest (ROI) were selected on the hypercube to calculate average reflectance spectra, including different sizes and portions of the FOV reporting identifiable visual features, e.g. blood clusters. This was done to investigate potential spatial changes in the reflectance spectra across the FOV of the samples. Examples of these spectra for one of the HGG samples are reported in Figure 8b, whereas the corresponding reflectance spectrum acquired with the spectrophotometer in the range 400-600 nm on the same biopsy is shown in Figure 8c.

Firstly, the comparison of the HyperProbe1 and the spectrophotometer data for the overlapping range between 510 and 600 nm showed significant consistency in both trends and shapes of the reflectance spectra, as well as in terms of absolute quantitative values. Subsequently, the comparison of the reflectance spectra on different ROIs for all the samples (both LLG and HGG) highlighted significant differences in their shapes and trends for two spectral ranges: (1)

Funded by the European Union
European Innovation Council

between 510 and 660 nm, and (2) between 780 and 880 nm. On the contrary, outside of these limited ranges, the rest of the spectral signatures demonstrated homogenous distribution of the optical properties of the samples across the whole examined FOVs. The largest differences were for the ROIs where visible concentrations of blood were present. This is consistent for the first mentioned range (510-600 nm), where the visible peaks of haemoglobin absorption are located. The enhanced absorption of haemoglobin could also explain differences in the spectra for the second mentioned range (780-880 nm), where the absorption spectrum of HbO_2 has a broad peak. However, differences were identified also for ROIs without visible blood clusters: this could then be connected to local differences in the concentrations of CCO, as the identified range overlaps with the NIR absorption peak of the latter.

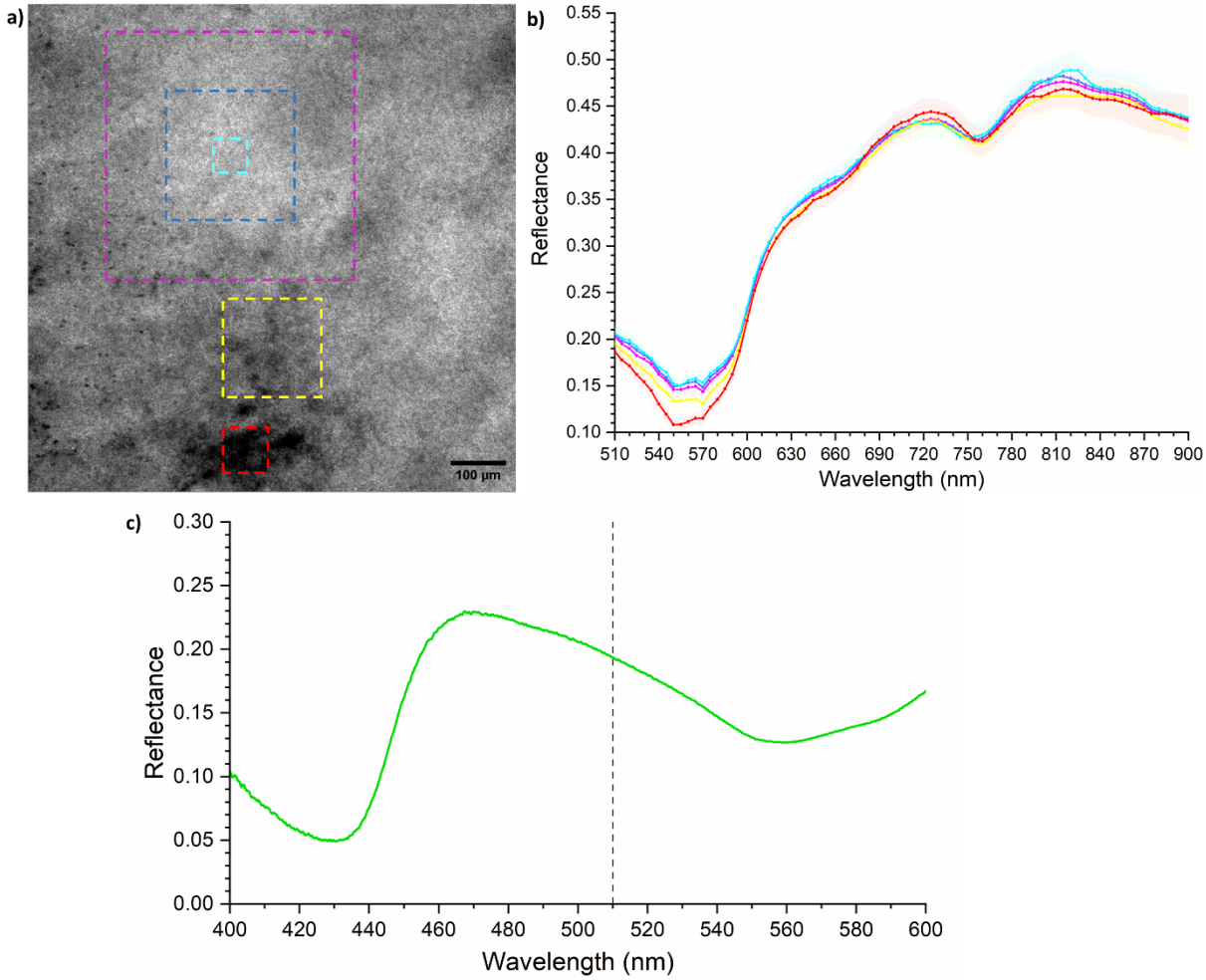

Fig. 8. *a) Processed spectral image of HGG biopsy sample acquired with the HyperProbe1 setup, at 560 nm, with selected ROIs in the FOV in which average reflectance spectra were calculated;*
b) Example of average reflectance spectra in the corresponding ROIs of the biopsy sample, for the whole hypercube;
c) Processed reflectance spectra of the same sample acquired with the spectrophotometer setup between 400 and 600 nm (highlighting the cut-off point at 510 nm with HyperProbe1).

Attenuation spectra, comprising of both the contribution of optical absorption and scattering, were then calculated from the reflectance spectra using the formula: A = -log10(R), where A and R are the attenuation and reflectance spectra, respectively. These attenuation spectra can provide a more direct comparison with the pure optical signatures of the chromophores of interest reported in Figure 7, as well as enable the identification of their potential influences and effects to the overall spectral signatures of the glioma tissue.

Figure 9a depicts an example of the average attenuation spectra of the same HGG sample, as in Figure 8a, and in the same selected ROIs. In the range 510-600 nm, the attenuation spectra of the HGG samples remarkably follow the combined shapes of the absorption spectra of HbO_2 and HHb, with discernible peaks at around 545-555 nm and at 575 nm. Another peak, from the absorption spectra of HHb, is also identifiable at around 755-760 nm. Particularly, attenuation in the range 510-600 nm appears to increase consistently when moving from the ROIs with no visible clustering of blood to the ROIs that includes the latter mostly or wholly, respectively. For the highlighted range between 780 and 900 nm, differences are reported for all the ROIs, regardless any visible features within them, with localised peaks of attenuation corresponding to around 840 nm, where the absorption of oxCCO is also at its highest. Specifically, variances among the concentric ROIs of different sizes in relatively homogenous areas of glioma tissue (with the largest changes appearing within the smallest ROIs) could be linked to either local variation in the abovementioned chromophore or to partial volume effects connected to changes in the optical pathlength of the sampled regions.

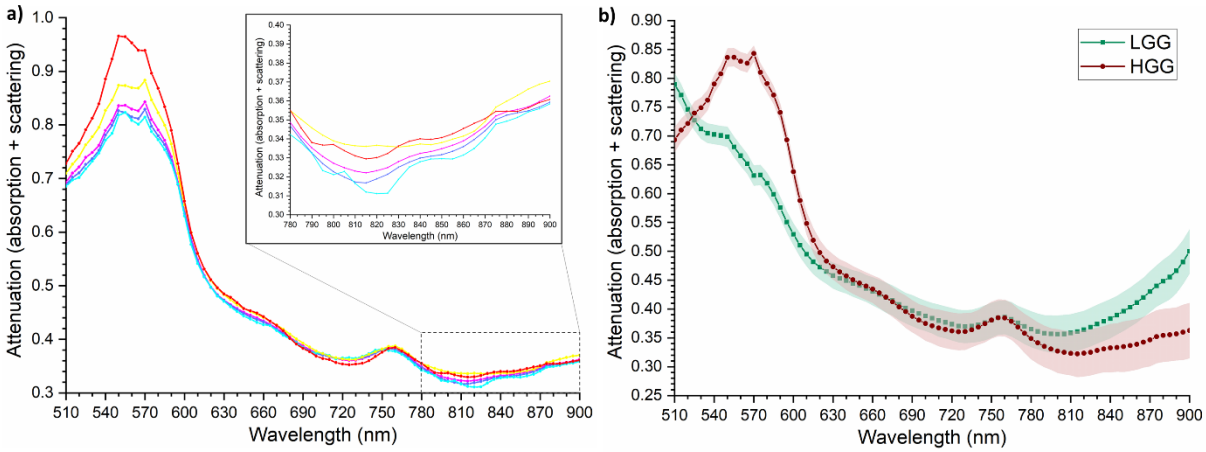

Fig. 9. *a) Example of average attenuation spectra in different ROIs of a HGG biopsy sample; b) Comparison of average attenuation spectra between LGG and HGG samples in selected similar, same-sized ROIs, for all the samples.*

The average attenuation spectra of the HGG and LGG samples across all the collected biopsies (n = 5) were then compared to each other, as reported in Figure 9b. Significant differences in specific intervals of the analysed spectral ranges emerge from the comparison, again with two major ranges of interest, i.e., 510-630 nm and 780-900 nm. LLG samples present lower attenuation and less identifiable features related to haemoglobin in the former range connected to the visible wavelengths, when compared to HGG biopsies. On the other hand, LGG show larger attenuation than HGG in the NIR range, albeit with a similar increasing and continuous trend.

5. Conclusions

The design and development of the laboratory version of the HyperProbe device, named HyperProbe1 has been extensively presented here, including initial characterisation and identification of potential limitations to overcome. The latter has led to the initiative of selecting and purchasing additional instrumentation to upgrade and optimise the final performances of the HyperProbe1 setup, which will then be investigated and tested in Task 1.3.

Preliminary application of the HyperProbe1 setup was also conducted on *ex vivo* fresh biopsies of glioma tissue for an initial study on the characterisation of its spectral features. The major outcome of this optical characterisation of glioma samples has demonstrated consistency between the high-resolution spectra obtained with the spectrophotometer and the data of the

Funded by the European Union
European Innovation Council

HyperProbe1 setup in the overlapping range of interest. This provide a very preliminary validation of the capability of the system, and of HSI in general, with a reduced number of discrete wavelength bands, to be able nonetheless to reconstruct optimally the optical features of *ex vivo* cerebral tissue. Further extension of this validation will then be required in the future to include also the portion of the electromagnetic spectrum above 600 nm.

Moreover, the preliminary results on both the HyperProbe1 and the spectrophotometer data have highlighted spectral signatures that can be directly linked to known chromophores in brain tissue, specifically the two forms of haemoglobin (HbO_2 and HHb) and CCO, which are critically involved in cerebral physiology and pathophysiology. In particular, differences between LLG and HHG samples have also emerged from the HyperProbe1 data, suggesting the potential for the setup to not only identify glioma tissue, but even provide differentiation in the severity and typology of the tumours themselves. Additional quantitative analysis and the application of advanced statistical approaches, such as machine learning techniques developed in WP4, will be explored in the near future, in order to corroborate these preliminary findings and establish a more objective and reliable methodology to extract key information and parameters from further HSI data acquired on the samples of glioma tissue, as part of Task 1.4 of WP1.

BIBLIOGRAPHY

[1] Lange F, Giannoni L, Tachtsidis I. The Use of Supercontinuum Laser Sources in Biomedical Diffuse Optics: Unlocking the Power of Multispectral Imaging. Appl Sci 2021;11:4616. https://doi.org/10.3390/APP11104616.

[2] Giannoni L, Lange F, Tachtsidis I. Hyperspectral imaging solutions for brain tissue metabolic and hemodynamic monitoring: past, current and future developments. J Opt 2018;20:044009. https://doi.org/10.1088/2040-8986/aab3a6.

[3] Giannoni L, Lange F, Sajic M, Smith KJ, Tachtsidis I. A hyperspectral imaging system for mapping haemoglobin and cytochrome-c-oxidase concentration changes in the exposed cerebral cortex. IEEE J Sel Top Quantum Electron 2021;27:7400411. https://doi.org/10.1109/JSTQE.2021.3053634.

[4] Lu G, Fei B. Medical hyperspectral imaging: a review. J Biomed Opt 2014;19:010901. https://doi.org/10.1117/1.JBO.19.1.010901.

[5] Della Puppa A, Munari M, Gardiman MP, Volpin F. Combined Fluorescence Using 5-Aminolevulinic Acid and Fluorescein Sodium at Glioblastoma Border: Intraoperative Findings and Histopathologic Data About 3 Newly Diagnosed Consecutive Cases. World Neurosurg 2019;122:e856–63. https://doi.org/10.1016/j.wneu.2018.10.163.

[6] SuperK FIANIUM - NKT Photonics n.d. https://www.nktphotonics.com/products/supercontinuum-white-light-lasers/superk-fianium/ (accessed August 30, 2023).

[7] SuperK SELECT - NKT Photonics n.d. https://www.nktphotonics.com/products/supercontinuum-white-light-lasers/superk-select/ (accessed August 30, 2023).

[8] PCO: pco.panda 4.2 n.d. https://www.pco-imaging.com/scientific-cameras/pcopanda-42/ (accessed August 30, 2023).

[9] OptoSpin 32 - Cairn Research n.d. https://www.cairn-research.co.uk/product/optospin32/ (accessed August 30, 2023).

[10] Noise Eaters / Laser Amplitude Stabilizers n.d. https://www.thorlabs.com/newgrouppage9.cfm?objectgroup_id=6107 (accessed August 30, 2023).

[11] Optotune - LSR-3005 Series n.d. https://www.optotune.com/index.php/products/laser-

Funded by the European Union
European Innovation Council

speckle-reducers/eap-lsr/lsr-3005-series.

[12] SuperK CONNECT - NKT Photonics n.d. https://www.nktphotonics.com/products/supercontinuum-white-light-lasers/superk-connect/ (accessed August 30, 2023).

[13] Wide Zoom Stereo Microscope | SZX16 | Olympus n.d. https://www.olympus-ims.com/en/microscope/szx16/#!cms[focus]=cmsContent11263 (accessed September 7, 2023).

[14] Thorlabs - Reflective Microscope Objectives n.d. https://www.thorlabs.com/newgrouppage9.cfm?objectgroup_id=6933.

[15] LabVIEW 2019 - National Instruments n.d. https://www.ni.com/it-it/shop/labview/labview-details.html.

[16] Spectralon® Diffuse Reflectance Targets n.d. https://www.labsphere.com/product/spectralon-reflectance-targets/ (accessed August 31, 2023).

[17] Jacques SL. Optical properties of biological tissues: a review. Phys Med Biol 2013;58:R37–61. https://doi.org/10.1088/0031-9155/58/11/R37.

[18] TwinFilm™ technology - SPECTROLIGHT Inc. n.d. https://www.spectrolightinc.com/board/detail/1/?board_id=132 (accessed September 1, 2023).

[19] XWS 65 - Broadband plasma light source n.d. https://www.isteq.nl/xws-65.php (accessed September 1, 2023).

[20] FWS-Poly - Flexible Wavelength Selector - SPECTROLIGHT Inc. n.d. https://www.spectrolightinc.com/shop/product/57 (accessed September 1, 2023).

[21] Giannoni L, Bonaudo C, Marradi M, Puppa A Della, Pavone FS. Optical characterisation and study of ex vivo glioma tissue for hyperspectral imaging during neurosurgery. Proc SPIE 12628, Diffus Opt Spectrosc Imaging IX 2023:153–9. https://doi.org/10.1117/12.2670854.

[22] Tungsten Halogen Light Source | HL-2000 | Ocean Insight n.d. https://www.oceaninsight.com/products/light-sources/vis-and-nir-light-sources/tungsten-halogen/ (accessed September 1, 2023).

[23] Flame Series General Purpose Spectrometers n.d. https://www.oceaninsight.com/blog/flame-series-general-purpose-spectrometers/ (accessed September 1, 2023).

[24] Bale G, Elwell CE, Tachtsidis I. From Jöbsis to the present day: a review of clinical near-infrared spectroscopy measurements of cerebral cytochrome-c-oxidase. J Biomed Opt 2016;21:091307. https://doi.org/10.1117/1.JBO.21.9.091307.